Supplementary information for "Orbital CO_2 reconstruction using boron isotopes during the late Pleistocene, an assessment of accuracy."

Elwyn de la Vega[ab], Thomas B. Chalk[ac], Mathis P. Hain[d], Megan R. Wilding[a], Daniel Casey[a], Robin Gledhill[a], Chongguang Luo[ae], Paul A. Wilson[a], Gavin L. Foster[a].

[a]School of Ocean and Earth Science, National Oceanography Centre Southampton, University of Southampton, Waterfront campus, Southampton SO14 3ZH, UK.
[b]University of Galway, Ollscoil na Gaillimhe, School of Geography, Archaeology & Irish Studies, University Road, Galway, H91 TK33, Ireland.
[c]Aix-Marseille Université, CNRS, IRD, INRAE, CEREGE, Aix-en-Provence, France
[d]Earth and Planetary Sciences, University of California, Santa Cruz, CA, USA.
[e]State Key Laboratory of Ore Deposit Geochemistry, Institute of Geochemistry, Chinese Academy of Sciences, Guiyang 550081, P.R. China.

Correspondence to Elwyn de la Vega: elwyn.delavega@universityofgalway.ie or elwyn.dlvega@gmail.com

Mg/Ca treatment	pH correction on Mg/Ca	Dissolution correction on Mg/Ca	Temperature calibration
Gray et al. (2018), global calibration "temperature only".	No	No	Mg/Ca = 1.26*exp(0.053*T)
Gray and Evans (2019), with pH correction.	Yes	No	Mg/Ca = exp(0.035*(S-35) + 0.064*T -0.87*(pH-8) - 0.03)
Gray et al. (2018) with dissolution correction on Mg/Ca.	No	Yes	Mg/Ca = 1.26*exp(0.053*T)
Gray end Evans (2019) with dissolution correction on Mg/Ca and pH correction.	Yes	Yes	Mg/Ca = exp(0.035*(S-35) + 0.064*T -0.87*(pH-8) - 0.03)
Anand et al. (2003).	No	No	Mg/Ca = 0.38*exp(0.09*T)
Anand et al. (2003) with dissolution correction.	No	Yes	Mg/Ca = 0.38*exp(0.09*T)

Table S1. Description of various *G. ruber* Mg/Ca treatments to assess the effect on calculated temperature and CO_2.

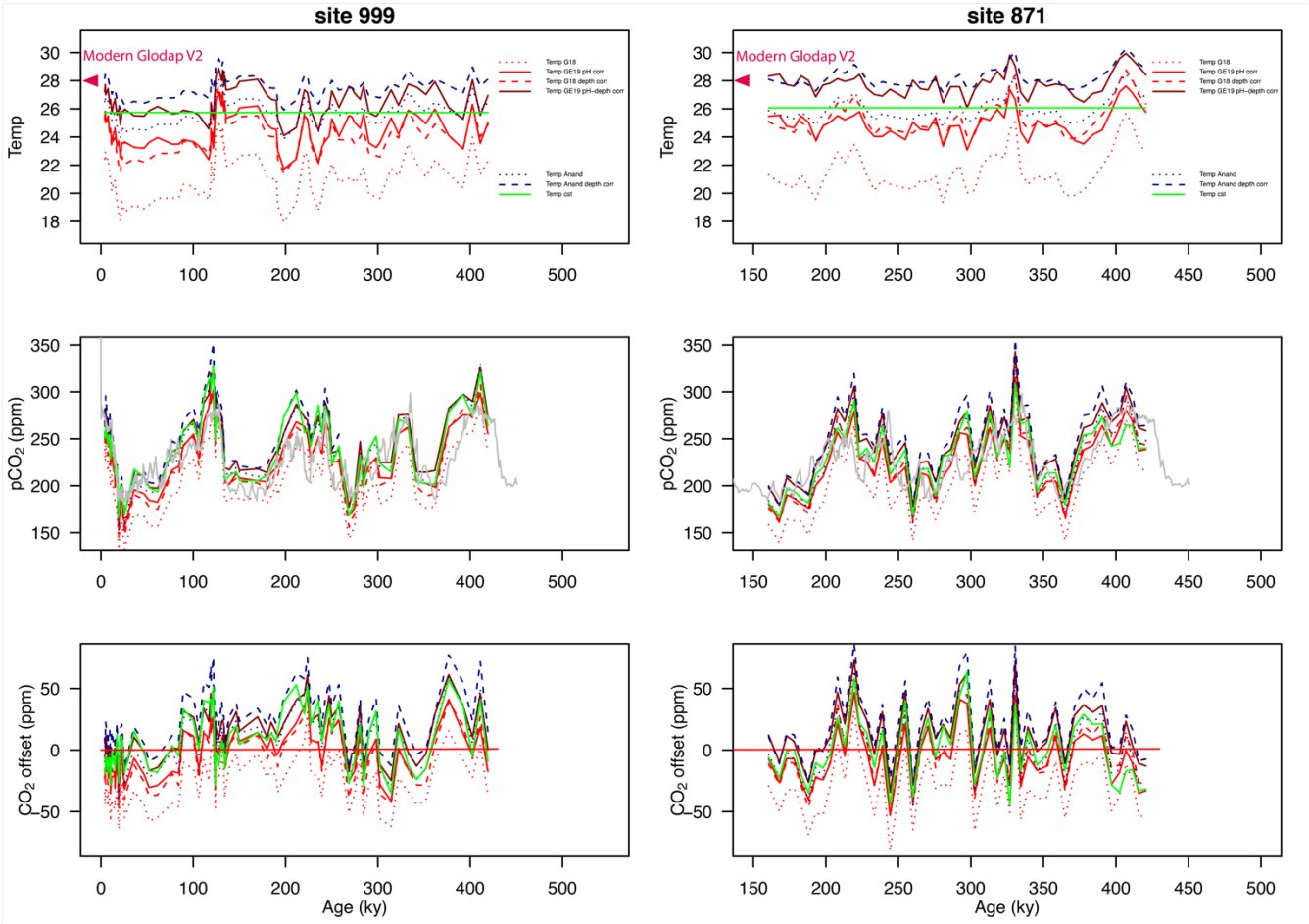

Figure S1. Effect of various temperature treatments (top), on δ^{11}B-derived CO_2 (middle) and CO_2 offset to the ice cores (bottom). Temperature treatments are: G18 (Gray et al., 2018, global calibration), GE19 pH corr (Gray and Evans 2019 with pH correction), G18 depth corr (Gray et al., 2018, with Mg/Ca corrected for depth/dissolution), GE19 pH-depth corr (Gray and Evans 2019, Mg/Ca corrected for depth/dissolution and corrected for pH), Anand (Anand et al., 2003, no correction), Anand depth corr (Anand et al., 2003, Mg/Ca corrected for depth/dissolution), Temp cst (constant temperature of 26°C). See Table S1 for description of temperature treatments. The red arrow in the top row is the modern temperature from Glodap v2 (Lauvset et al., 2022) for each site. Note the coretop temperature at 871 is not displayed and the most recent Mg/Ca from Dyez and Ravelo. (2013) was used.

Mg/Ca treatment	core	CO2 offset	2sd	core	CO2 offset	2sd	Average CO2 offset for both records
T Gray18	999	-27.03	40	871	-28.21	52	-27.62
T GE19 pH corr	999	-3.87	39	871	-6.40	47	-5.14
T Gray18 depth corr	999	-6.77	43	871	-3.30	54	-5.03
T GE19 pH corr, depth corr	999	12.06	41	871	13.89	51	12.98
T Anand03	999	6.64	45	871	1.37	54	4.00
T Anand03 depth corr	999	23.28	48	871	20.88	57	22.08
T constant	999	6.33	46	871	0.23	53	3.28

Table S2. Effect of various Mg/Ca-derived temperature calibrations on CO_2 offset (ppm). See Figure S1 for descriptions of Mg/Ca treatments.

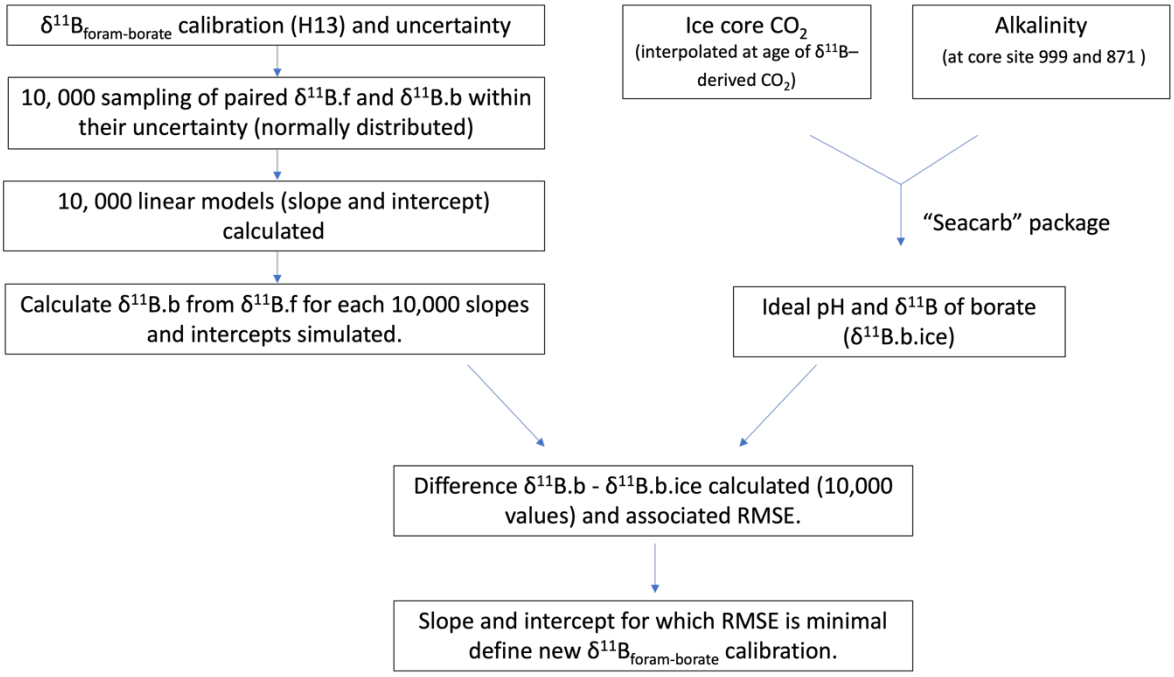

Figure S2. Optimisation of the borate-foram $\delta^{11}B$ calibration by minimising the RMSE (root mean squared error) between the $\delta^{11}B$ of borate derived from ice core CO_2, and the $\delta^{11}B$ of borate simulated from 10,000 slopes and intercept. The slopes and intercept are simulated within the uncertainty of $\delta^{11}B$ borate and pH calibration (H13) of Henehan et al. (2013). $\delta^{11}B.f$, $\delta^{11}B.b$ and $\delta^{11}B.b.ice$ are for $\delta^{11}B$ of foraminifera, borate and borate derived from the ice cores, respectively.

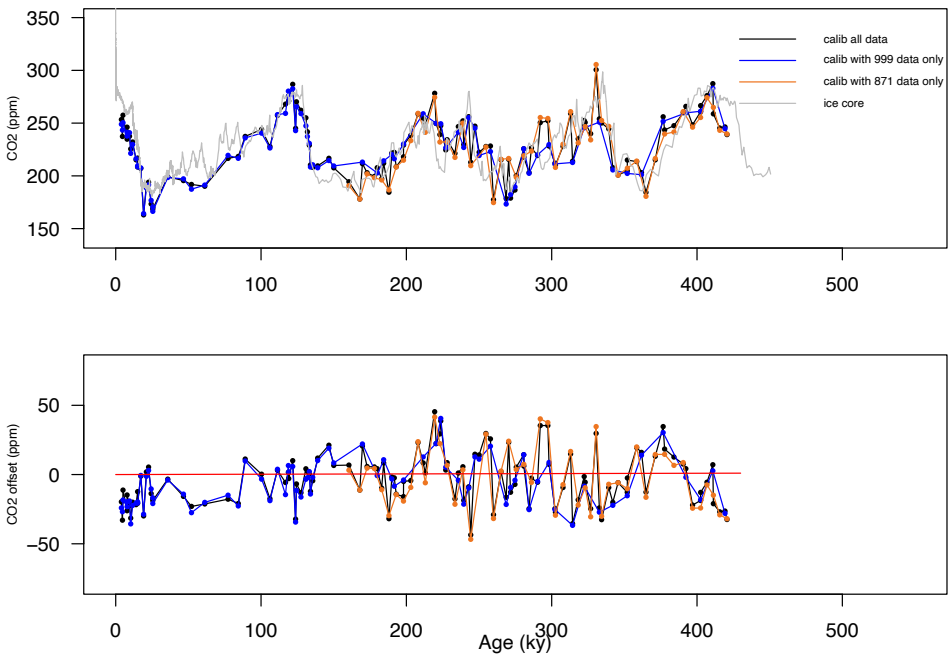

Figure S3. All $\delta^{11}B$-derived CO_2 (top) and resulting CO_2 offset (bottom) calculated with the optimised calibrations using the combined data set from both cores 999 and 871 (black) and each separate data set from site 999 (blue) and 871 (orange).

Downcore calibration	Slope	Intercept	Average CO2 offset (ppm)
All data	0.713	6.492	4
999 only	0.724	6.326	-7
871 only	0.710	6.532	-3

Table S3. Slope, intercept and average CO_2 offsets values for different optimised calibrations presented in Figure S3.

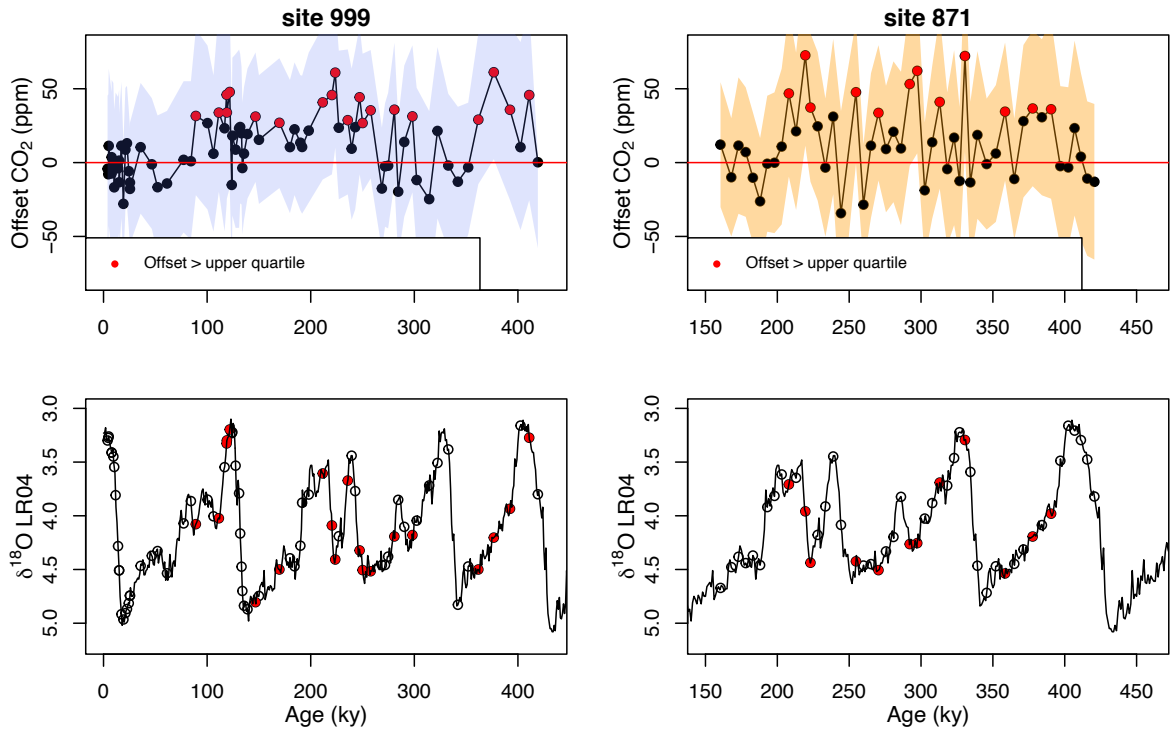

Figure S4. Upper panel: CO_2 offset ($\delta^{11}B$-derived CO_2 minus ice core CO_2), red dots are the offset above the upper quartile (i.e. 25% of the data that lies above the upper quartile). Lower panel: LR04 $\delta^{18}O$ (black line), interpolated $\delta^{18}O$ (open circles) from the $\delta^{11}B$-derived CO_2 and red points are the interpolated values for which CO_2 offset is high (above the upper quartile). This shows that the values of high CO_2 offset (between boron-derived and ice core CO_2) tend to fall within periods at the beginning of the glaciation.

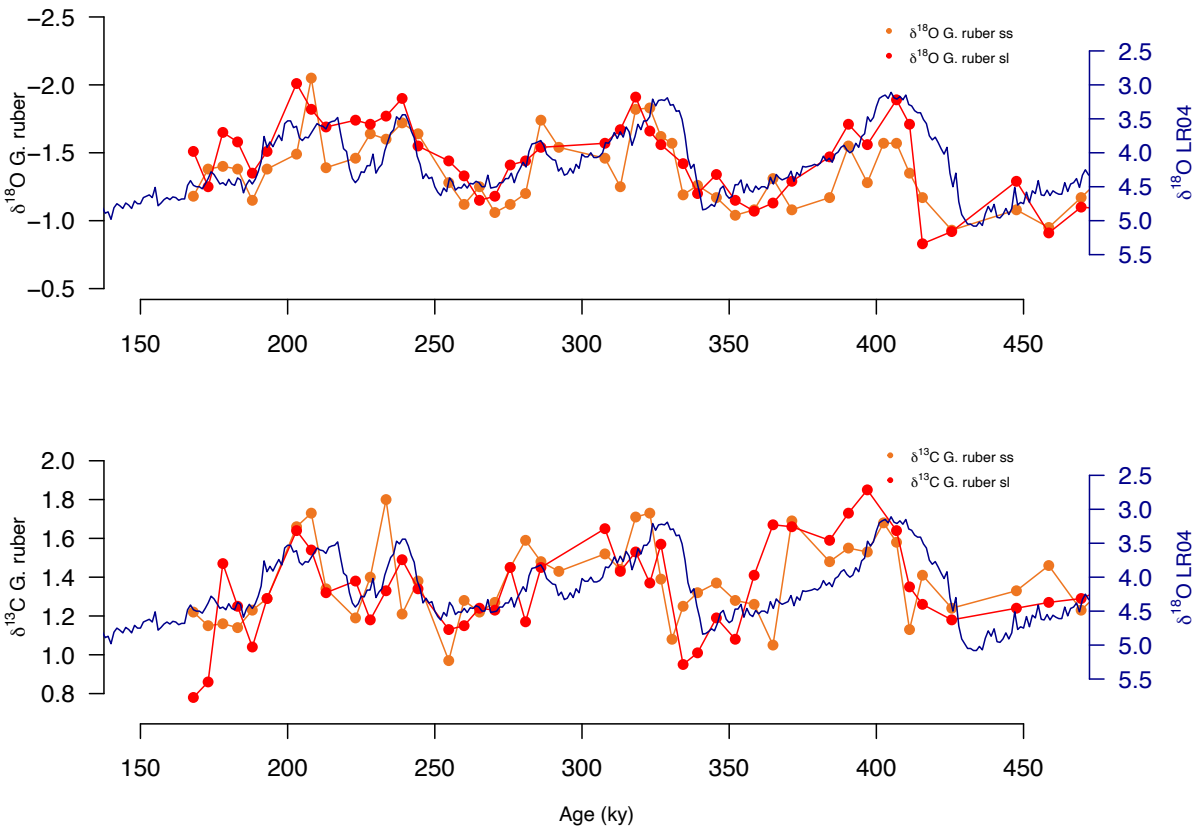

Figure S5. Time series of $\delta^{13}C$ and $\delta^{18}O$ for the two morphotypes of *G. ruber* at ODP Site 871 (sensu stricto, orange; and sensu lato, red). The benthic $\delta^{18}O$ stack LR04 is plotted for reference (dark blue).

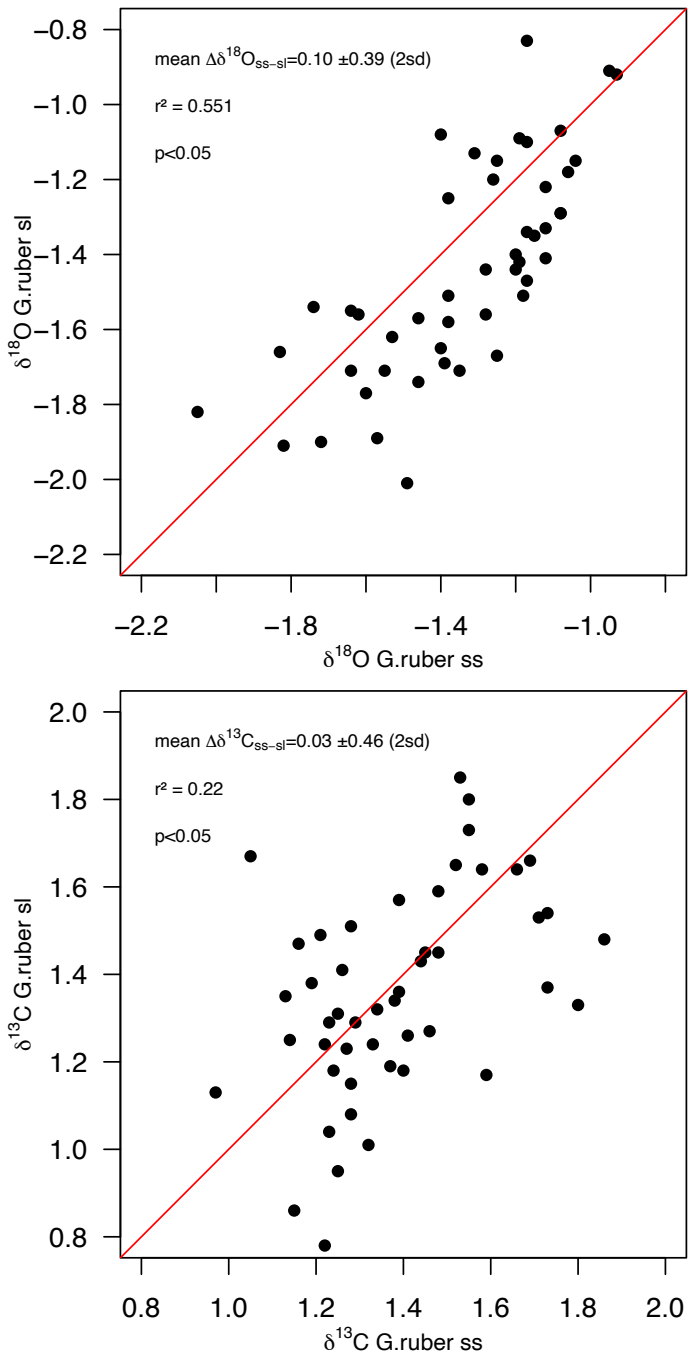

Figure S6. Cross plot of $\delta^{18}O$ and $\delta^{13}C$ of the two morphotypes of *G. ruber* (*sensu stricto* and *sensu lato)* from ODP site 871, and associated r^2 . The red line is the 1:1 line. The mean offset and 2 standard deviation (sd) between $\delta^{18}O$ and $\delta^{13}C$ of both morphotypes are shown (‰).

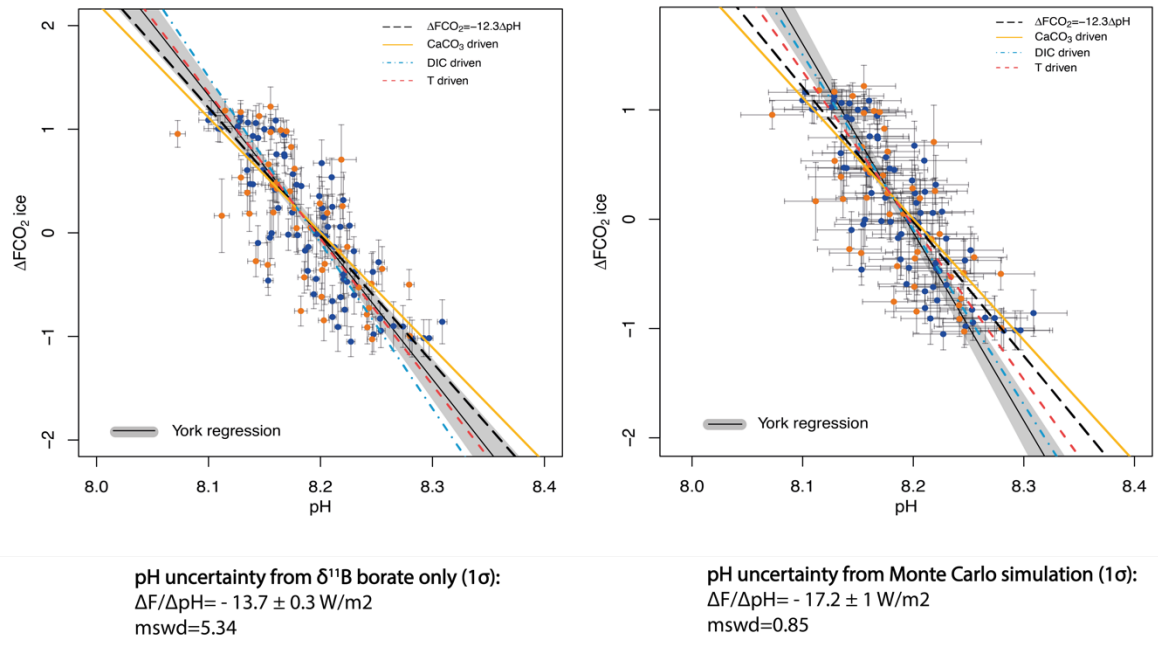

Figure S7. Effect of pH uncertainty on the York regression between ΔFCO_2 and pH for site 999 (blue dots) and 871 (orange dots). goodness of fit MSWD is improved when using the fully propagated pH uncertainty (derived from the Monte Carlo simulation).

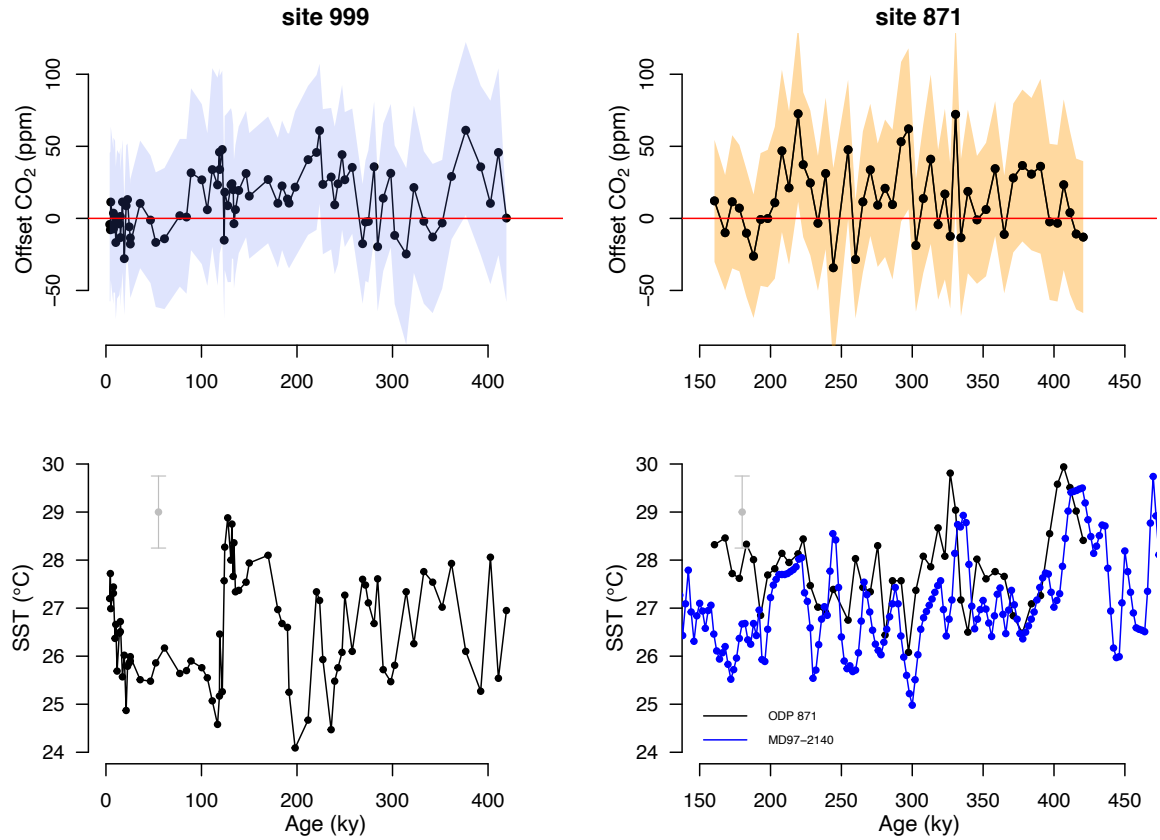

Figure S8. CO_2 offset (δ^{11}B-derived CO_2 minus ice core CO_2) compared to Mg/Ca-derived sea surface temperature of *G. ruber* (left ODP Site 999, right ODP Site 871) and SST from the stratified equatorial West Pacific core MD97-2140 (de Garidel-Thoron et al., 2005). Periods of high CO_2 offset do not coincide with anomalous cold temperature recorded by *G. ruber*, ruling out upwelling and CO_2 disequilibrium as a cause of CO_2 offsets.

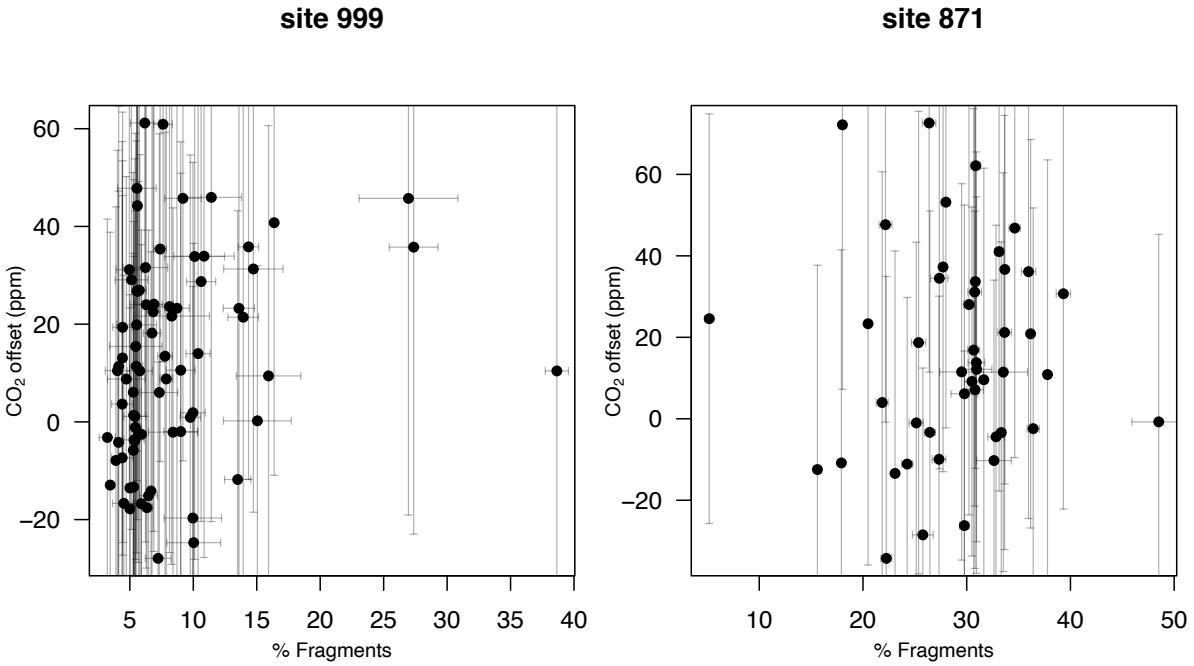

Figure S9. Cross plot of CO_2 offset (difference between CO_2 calculated from $\delta^{11}B$ and from the ice core record) and fragment counts at Site 999 (left) and 871 (right). Fragmentation index at Site 999 (Schmidt et al. 2006) are interpolated from $\delta^{11}B$-derived CO_2. Fragmentation index and $\delta^{11}B$-derived CO_2 are from the same sample at Site 871. Ice core CO_2 data are interpolated from $\delta^{11}B$-derived CO_2 at both sites.

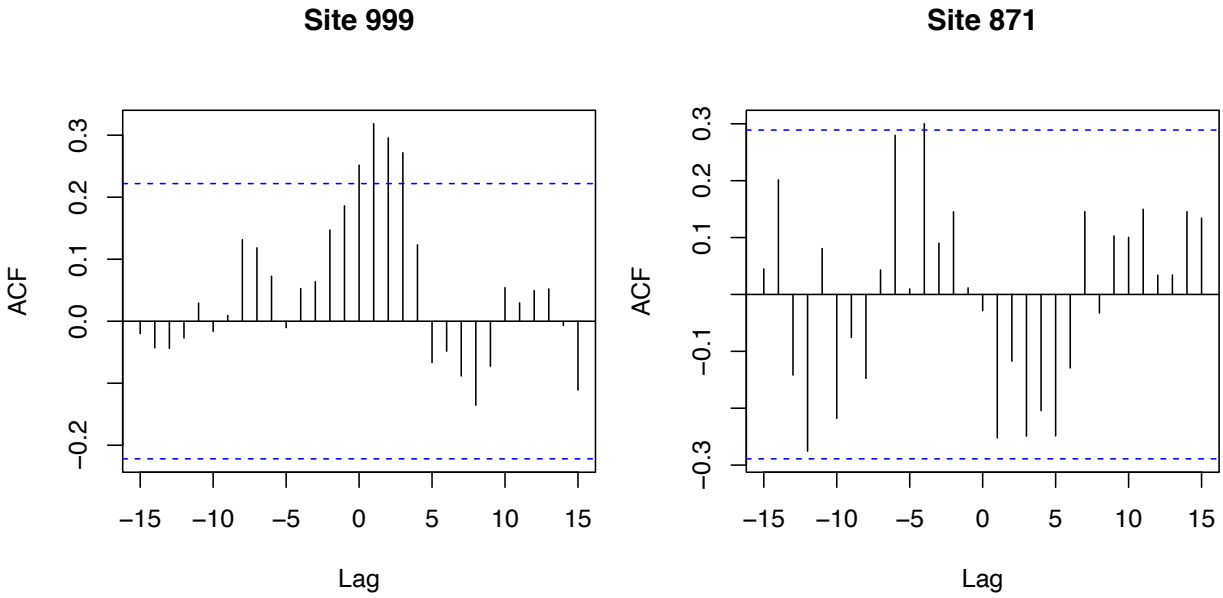

Figure S10. Cross-corelation function of CO_2 offset and fragmentation index for Site 871 and 999 for various lags. Negative (positive) lags mean that CO_2 offset leads (lag) fragmentation index. The blue dotted lines are uncertainties (95% confidence), the values beyond which the autocorrelation (ACF) is significant. The lag represents the number of points in time by which a time series is lagged from the other. For the lag window inspected here (with an average time difference of 5.4 and 5.7 ky between points for site 871 and 999 respectively) , most correlations between CO_2 offset and fragmentation index are effectively 0 (except 4 values at site 999 showing a week ACF bellow 0.3 for lags between 0 and 3 sample/time points) which argues in favour of no correlation between CO_2 offset and fragmentation index.

Supplementary information S11. Relationship between pH, DIC and TA.

Dissolved inorganic carbon DIC and total alkalinity TA, are defined by the following, with [X] the concentration of compound X.

$$DIC = [CO_2] + [HCO_3^-] + [CO_3^{2-}] \text{ (eq 1a)}$$

$$TA = [HCO_3^-] + 2[CO_3^{2-}] + [B(OH)_4^-] + [OH^-] - [H^+] + minor\ compounds \text{ (eq 2a)}$$

At pH 8.1 in seawater CO_2 concentrations is small, such as equation (1a) can be approximated to:

$$DIC = [HCO_3^-] + [CO_3^{2-}] \text{ (eq 1b)}$$

TA can also be approximated by the carbonate alkalinity such as:

$$TA = [HCO_3^-] + 2[CO_3^{2-}] \text{ (eq 2b)}$$

By combining (eq1b) and (eq2b), we obtain:

$$TA - DIC = [CO_3^{2-}] \text{ (eq3)}$$
$$2DIC - TA = [HCO_3^-] \text{ (eq4)}$$

Now considering the equilibrium constants of carbonate compounds in seawater from the following chemical reactions (K_1 and K_2 are the equilibrium constants):

$$CO_2 + H_2O \Leftrightarrow [HCO_3^-] + [H^+] \text{ } (K_1)$$
$$[HCO_3^-] \Leftrightarrow [CO_3^{2-}] + [H^+] \text{ } (K_2)$$

$$\text{With } K_1 = \frac{[HCO_3^-][H^+]}{[CO_2]} \text{ (eq5)}$$

$$K_2 = \frac{[CO_3^{2-}][H^+]}{[HCO_3^-]} \text{ (eq6)}$$

It follows from (eq6), (eq3) and (eq4):

$$[H^+] = \frac{K_2(2DIC - TA)}{TA - DIC} \text{ (eq7)}$$

As pH is related to [H+], any change in alkalinity for a given pH, is compensated by a change in DIC.

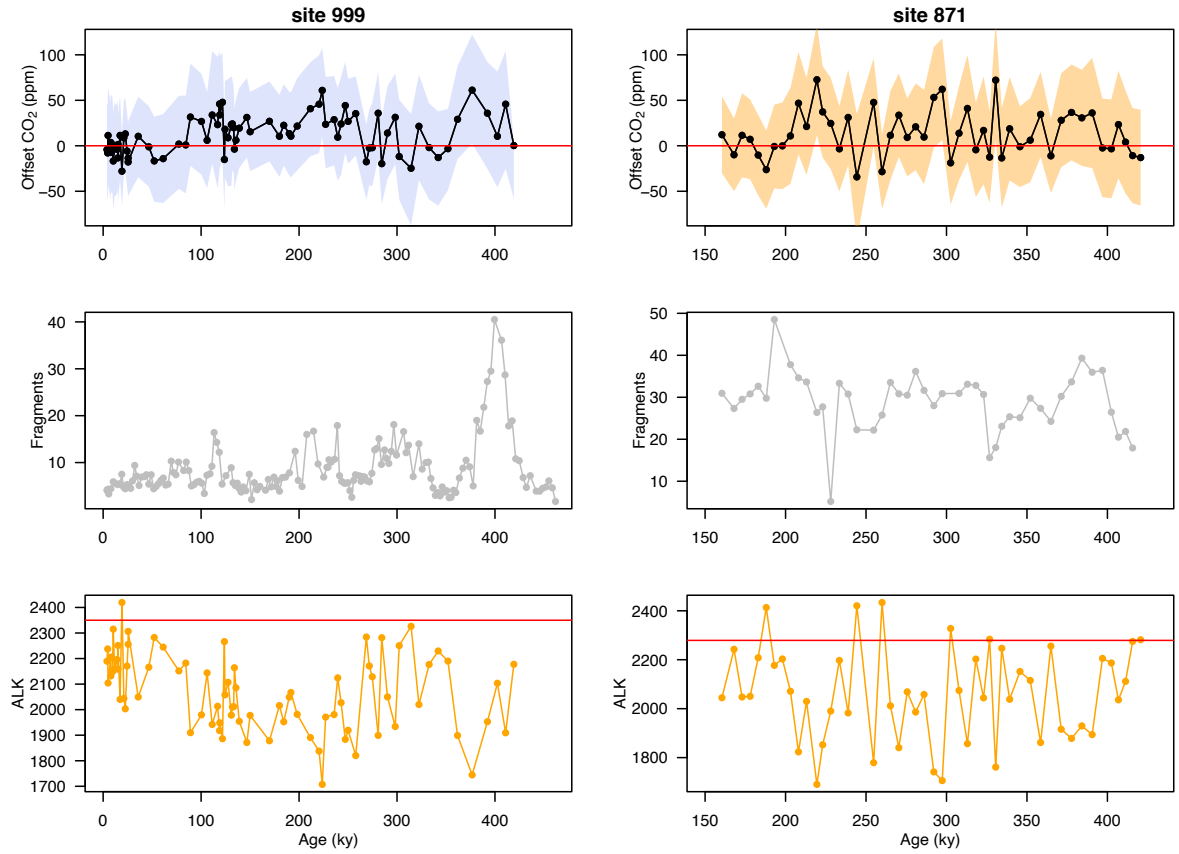

Figure S12 . Left column: ODP Site 999, right column: ODP Site 871. Alkalinity (ALK, µmol/kg) change calculated from δ^{11}B-derived pH and ice core CO_2. The red line is the modern alkalinity values at each core site. If CO_2 offsets were only produced by alkalinity change, it would require an alkalinity change of up to 500 µmol/kg, a value beyond any estimated changes over the late Pleistocene (Hönisch et al., 2009, Cartapanis et al., 2018).

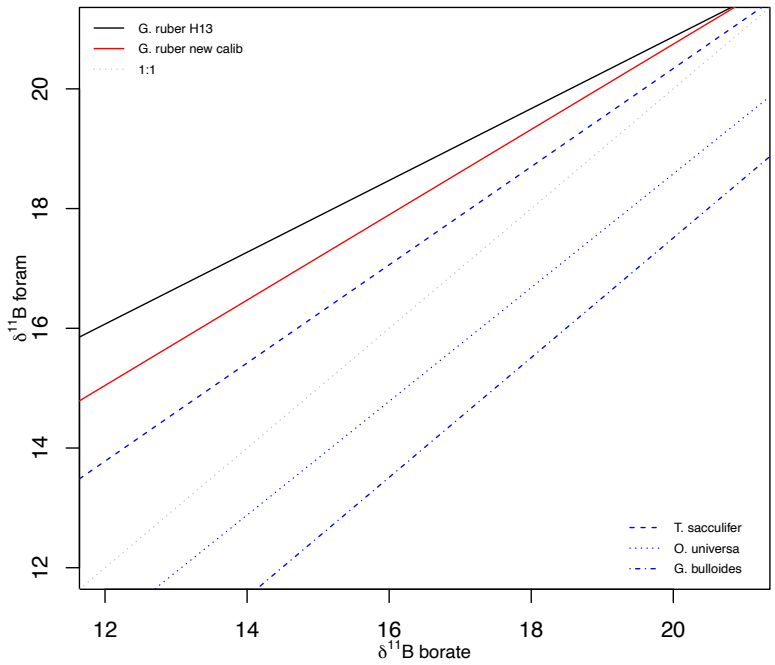

Figure S13. Comparison of the optimised $\delta^{11}B$ foram/borate calibration with the published calibration slope of Henehan et al. (2013) along with other calibration slopes of spinose foraminifera *T. sacculifer* (Martínez-Botí et al., 2015), *O. universa* (Henehan et al., 2016) and *G. bulloides* (Martínez-Botí et al., 2015).

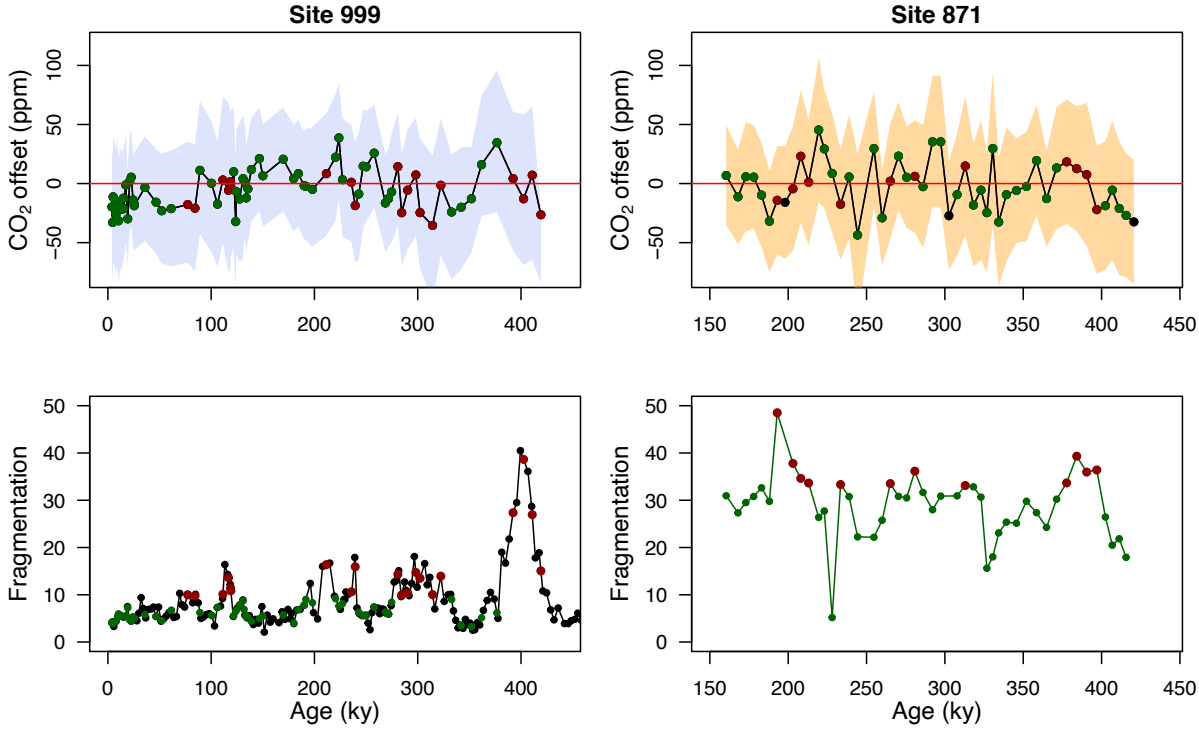

Figure S14. CO_2 offset (coloured dots, defined as $\delta^{11}B$-derived CO_2 minus ice core CO_2) with optimised borate-foram $\delta^{11}B$ calibration. Lower panels: fragmentation index. Red dots in the lower panels are the fragments above the upper quartile (and corresponding CO_2 in the upper panel, red dots). Green dots represent periods of low fragments below the upper quartile (and corresponding CO_2 in the upper panel, green dots).